

**An efficient implementation of
boundary element methods
for computationally expensive
Green's functions**

Daan Huybrechs and Stefan Vandewalle

Report TW 510, November 2007



Katholieke Universiteit Leuven
Department of Computer Science
Celestijnenlaan 200A – B-3001 Heverlee (Belgium)

An efficient implementation of boundary element methods for computationally expensive Green's functions

Daan Huybrechs and Stefan Vandewalle

Report TW 510, November 2007

Department of Computer Science, K.U.Leuven

Abstract

We describe an implementation technique for boundary element methods that greatly reduces the required number of evaluations of the Green's function. Assuming that evaluating the Green's function is a costly operation, our approach has a computational cost that is almost independent of the chosen discretization scheme. Nyström methods, collocation methods and Galerkin methods lead to similar computation times, although the latter requires the computation of a large number of double integrals. The result is obtained mainly by constructing a specific family of quadrature and cubature rules that maximizes the possibility of sharing function evaluations.

We apply the technique to the problem of scattering of electromagnetic waves by diffraction gratings in two dimensions. In this case the Green's function is given by a slowly converging oscillatory series. We describe a novel approach for evaluating such series and we illustrate our implementation with numerical results.

Keywords : integral equations, numerical integration, oscillatory series
AMS(MOS) Classification : Primary : 65N38, Secondary : 65D30, 65B10.

An efficient implementation of boundary element methods for computationally expensive Green's functions

Daan Huybrechs and Stefan Vandewalle

Katholieke Universiteit Leuven
Department of Computer Science
Celestijnenlaan 200A, B-3001 Leuven, Belgium.
{Daan.Huybrechs,Stefan.Vandewalle}@cs.kuleuven.be

Abstract

We describe an implementation technique for boundary element methods that greatly reduces the required number of evaluations of the Green's function. Assuming that evaluating the Green's function is a costly operation, our approach has a computational cost that is almost independent of the chosen discretization scheme. Nyström methods, collocation methods and Galerkin methods lead to similar computation times, although the latter requires the computation of a large number of double integrals. The result is obtained mainly by constructing a specific family of quadrature and cubature rules that maximizes the possibility of sharing function evaluations.

We apply the technique to the problem of scattering of electromagnetic waves by diffraction gratings in two dimensions. In this case the Green's function is given by a slowly converging oscillatory series. We describe a novel approach for evaluating such series and we illustrate our implementation with numerical results.

1 Introduction

Numerical integration plays an important role in several discretization schemes for the numerical solution of integral equations. The calculations typically involve integrals of a Green's function that has a singular behaviour. In so-called Nyström methods, the need for numerical integration is entirely avoided [5]. Each element of the discretization matrix or coupling matrix consists of just one evaluation of the Green's function for a certain source point and field point. One solves the resulting set of equations to find the point values of the solution. In collocation methods, or point-matching methods, the solution is sought as a linear combination of certain basis functions. Each element of the coupling matrix consists of an integral involving the Green's function and one such basis function [4]. Finally, in Galerkin methods, the approximate solution of the integral equation is tested by integrating with respect to certain test functions, rather than by point matching. This leads to a double integration for each element, one with the Green's function and the basis functions (commonly called trial functions) and another one with the test functions. Both collocation methods and Galerkin methods can be seen as different realizations of the Method of Moments [9].

For two-dimensional problems, each integration is one-dimensional. Thus, the collocation method requires the evaluation of a large number of single integrals, some of which may be

singular. Galerkin methods require the evaluation of double integrals, that are possibly singular as well. For a matrix of size N by N , one has to evaluate N^2 such integrals. On the other hand, the Nyström method requires just N^2 evaluations of the Green's function, with some care at the singularity. The differences in the computational cost of these methods is reflected in the accuracy of the solution. It depends of course on the application whether or not high accuracy is required. The most common choice in implementations is a collocation method, i.e., the Method of Moments combined with point-matching. The reasonable assumption is that Galerkin methods are computationally too expensive for numerical simulations.

It is the purpose of this paper to challenge this assumption. We will show that both collocation and Galerkin discretizations can be constructed at a cost that is roughly equal to the cost of a straightforward Nyström discretization. This is particularly the case when each evaluation of the Green's function is a costly operation.

The result is obtained by constructing suitable quadrature rules that are tailored to the basis functions and to the type of singularity of the Green's function. Explicit formulas for their construction are provided. We apply the technique to the problem of scattering by diffraction gratings. There, the Green's function is a quasi-periodic function that is given by a slowly convergent series with oscillatory terms. First, we describe a new method for the efficient evaluation of the series. Whereas several million terms of the original series are required for a reasonable accuracy, in our approach typically 50–300 terms are sufficient to reach machine precision. Still, this is 300 times more expensive than the evaluation of a Green's function that is given by a single well-known special function, such as the Hankel function. Next, we show that the total number of evaluations in our Galerkin implementation is roughly equal to N^2 , only one per element of the coupling matrix.

The description of our method is rather general. Still, we do not make the claim that collocation or Galerkin methods can always be implemented as efficiently as in this fairly simple, yet certainly non-trivial, application. The result relies on certain assumptions, one of them being that the equation is discretized on a regular grid. A second assumption is that all basis functions are shifted versions of one another (for example, pulse functions or hat functions). Although these assumptions are certainly reasonable for two-dimensional problems, they may become exceedingly unrealistic in three dimensions. We do note that both assumptions are not absolutely essential. They could be alleviated, at least in principle, at the cost of having to compute a larger number of quadrature rules a priori. We will make no attempt at such generalization in this paper. Finally, we note that even if the assumptions are not satisfied for all basis functions or for the entire discretization, large savings can still be obtained if the described approach can be applied to a significant portion of the discretization matrix.

We start the paper with a brief overview of different discretization schemes in Section 2. We describe a technique for evaluating the off-diagonal entries of the discretization matrices in Section 3. These correspond to non-singular integrals. The efficient evaluation of diagonal entries, involving singular integrals, is discussed in Section 4. We describe the scattering by diffraction gratings in Section 5 and we end with some numerical results in Section 6.

2 Discretization schemes for boundary integral equations

In this section, we formulate three different discretization schemes for integral equations. We consider integral equations on the boundary $\Gamma := \partial\Omega \subset \mathbb{R}^2$ of a two-dimensional volume Ω .

For simplicity of notation, we consider only integral equations of the first kind of the form

$$\int_{\Gamma} G(\mathbf{x}, \mathbf{y}) u(\mathbf{y}) \, ds_{\mathbf{y}} = f(\mathbf{x}), \quad \mathbf{x} \in \Gamma, \quad (2.1)$$

but the quadrature approach is equally valid for integral equations of the second kind,

$$\lambda u(\mathbf{x}) + \int_{\Gamma} G(\mathbf{x}, \mathbf{y}) u(\mathbf{y}) \, ds_{\mathbf{y}} = f(\mathbf{x}), \quad \mathbf{x} \in \Gamma, \quad \lambda \neq 0.$$

For time-harmonic and transverse-magnetic (TM) polarized electromagnetic waves, Maxwell's equations reduce to the Helmholtz equation

$$\Delta u + k^2 u = 0.$$

The solution to the boundary value problem $u(\mathbf{x}) = 0$ on the boundary Γ can be found from the solution of the integral equation (2.1). Here, $f(\mathbf{x})$ is the incoming wave and the solution $u(\mathbf{y})$ is proportional to the induced current on the boundary Γ of a perfectly conducting scattering obstacle [5, 9]. The Green's function $G(\mathbf{x}, \mathbf{y})$ is in this case given by

$$G(\mathbf{x}, \mathbf{y}) = \frac{i}{4} H_0^{(1)}(k|\mathbf{x} - \mathbf{y}|), \quad (2.2)$$

where $H_0^{(1)}(z)$ is the Hankel function of the first kind and order zero. We will frequently use (2.2) to illustrate some elements of our approach further in the paper.

Assume for simplicity that a single periodic parameterization $\kappa : [0, 1] \rightarrow \Gamma$ exists for the boundary Γ . The solution $u(\mathbf{y})$ of equation (2.1) is then sought in the form

$$u(\kappa(\tau)) = \sum_{n=1}^N c_n \phi_n(\tau), \quad \tau \in [0, 1],$$

for a given set of basis functions $\{\phi_n\}$ that are defined on the parameter domain $[0, 1]$. We will denote the support of the basis functions ϕ_n by $\Omega_n := [a_n, b_n] \subset [0, 1]$.

Galerkin method. The Galerkin discretization for equation (2.1) leads to a dense linear system $A_g x = b_g$ with the entries of the discretization matrix A_g given by

$$A_g^{m,n} = \int_{\Omega_m} \int_{\Omega_n} G(\kappa(t), \kappa(\tau)) \phi_n(\tau) \phi_m(t) |\kappa'(\tau)| |\kappa'(t)| \, d\tau \, dt, \quad (2.3)$$

and the elements of the right hand side vector b_g given by

$$b_g^m = \int_{\Omega_m} f(\kappa(t)) \phi_m(t) |\kappa'(t)| \, dt,$$

where we have chosen the test functions $\{\phi_m\}$ identical to the trial functions $\{\phi_n\}$.

Collocation method. The collocation approach replaces the integration with the test functions $\phi_m(t)$ by point evaluations in a set of collocation points $t_m \in [0, 1]$, $m = 1, \dots, N$. This leads to a dense linear system $A_c x = b_c$, with the matrix entries given by

$$A_c^{m,n} = \int_{\Omega_n} G(\kappa(t_m), \kappa(\tau)) \phi_n(\tau) |\kappa'(\tau)| \, d\tau. \quad (2.4)$$

The computation of the right hand side vector b_c reduces to the function evaluations $b_c^m = f(t_m)$, $m = 1, \dots, N$.

Nyström method. The simplest discretization for (2.1) consists of only evaluating the Green's function at certain points $(x_m, y_n) \in \mathbb{R}^2 \times \mathbb{R}^2$, $n, m = 1, \dots, N$. This discretization can be obtained by using a one-point quadrature rule for the integral in (2.4), and using pulse basis functions

$$\phi_n(\tau) = \begin{cases} 1, & t \in [\frac{n-1}{N}, \frac{n}{N}], \\ 0 & \text{otherwise,} \end{cases} \quad n = 1, \dots, N.$$

It leads to a dense linear system $A_p x = b_p$, with matrix entries given by

$$A_p^{m,n} = G(\kappa(t_m), \kappa(t_n)) |\kappa'(t_n)| |\Omega_n|, \quad n \neq m,$$

where $|\Omega_n|$ is the size of the support of ϕ_n . The right hand side is the same as in the collocation case, $b_p = b_c$. Point evaluation is not possible for the entries on the diagonal where $m = n$, due to the singularity of the kernel function when $x = y$. Various approaches exist to overcome this difficulty, we refer the reader to [9].

The discretization matrix A_p only requires approximately N^2 evaluations of the Green's function for computing all N^2 entries of the matrix, and is hence the cheapest discretization of the three schemes considered.

3 The efficient evaluation of off-diagonal entries

First, we describe an efficient implementation for computing the off-diagonal elements of the discretization matrices. Since the evaluation of the Green's function is considered to be costly, a scheme is developed where those function evaluations are maximally shared. A suitable quadrature rule is constructed for one-dimensional integrals arising in the collocation scheme in §3.1. A method for double integrals that appear in the Galerkin scheme is obtained by a tensor product application of the one-dimensional rule in §3.4. The scheme for one-dimensional integrals is essentially based on an idea that was originally proposed in the context of wavelet applications [16].

3.1 Suitable quadrature for one-dimensional integrals

The integrals that arise in the collocation method, given in expression (2.4), have the form

$$I_n = \int_{a_n}^{b_n} f(\tau) \phi_n(\tau) d\tau, \quad n = 1, \dots, N, \quad (3.1)$$

with

$$f(\tau) = G(\kappa(t_m), \kappa(\tau)) |\kappa'(\tau)|. \quad (3.2)$$

The function $f(\tau)$ is a smooth function unless the integration domain contains the collocation point t_m , in which case f is singular, or if the boundary Γ has corners, in which case f is not differentiable at the corner points. The basis functions ϕ_n are not necessarily smooth functions. They can be piecewise smooth, as is the case for piecewise linear functions and more general spline functions, or not very smooth at all, as may be the case when using

wavelets. A classical quadrature rule for (3.1), with weights $w_{n,j}$ and points $x_{n,j} \in \Omega_n$, would lead to the approximation

$$I_n \approx \sum_{j=0}^r w_{n,j} f(x_{n,j}) \phi_n(x_{n,j}). \quad (3.3)$$

If the points $x_{n,j}$ for all I_n are distributed on a regular grid of $[0, 1]$, then the costly function evaluations $f(x_{n,j})$ can be shared among the evaluations of $I_{n-1}, I_n, I_{n+1}, \dots$ involving neighbouring basis functions. This leads one to consider so-called Newton-Cotes quadrature rules (see [8, §2.5]), since these quadrature rules employ equispaced quadrature points:

$$x_{n,j} := a_n + j \frac{b_n - a_n}{r}.$$

Newton-Cotes quadrature rules would not yield good results for the approximation (3.3) however, because the integrand $f(\tau)\phi_n(\tau)$ is not smooth. These rules are based on polynomial interpolation of the integrand, and hence they will only give an accurate approximation if the integrand can be approximated well by a polynomial.

Newton-Cotes quadrature rules can also be constructed for a weight function $w(x)$,

$$\int_a^b w(x) f(x) dx \approx \sum_{j=0}^r w_j f(x_j), \quad \text{with } x_j := a + j \frac{b-a}{r}, \quad (3.4)$$

such that only evaluations of $f(x)$ are required in the application of the rule. Moreover, $w(x)$ is not required to be smooth, and the accuracy of the approximation only depends on the smoothness of $f(x)$. Hence, the solution to the lack of smoothness of the integrand of the collocation integral (3.1) is to include the basis function $\phi_n(x)$ into the weight function. This idea was proposed in [16] and extended in [10] in the context of wavelet applications.

Let us first assume that all basis functions are shifted versions of one mother basis function $\phi(\tau)$ defined on the interval $[a, b]$, such that

$$\phi_n(\tau) := \phi(N\tau - n), \quad \text{and} \quad [a_n, b_n] := \left[\frac{a+n}{N}, \frac{b+n}{N} \right], \quad (3.5)$$

with a and b integers. This property holds for almost all basis functions that are defined on a regular grid. The integers that lie in the interval $[a, b]$ typically correspond to certain points of discontinuity of the basis functions. For example, the hat function can be defined on $[-1, 1]$ with the peak value at the integer 0, as shown in Figure 1. More generally, for B-splines the integers correspond to the knots of the spline. With the substitution $x = N\tau - n$, the integrals (3.1) take the form

$$I_n = \frac{1}{N} \int_a^b f\left(\frac{x+n}{N}\right) \phi(x) dx.$$

They can be approximated by

$$I_n \approx \frac{1}{N} \sum_{j=0}^r w_j f\left(\frac{x_j+n}{N}\right), \quad (3.6)$$

where the quadrature points x_j are given by (3.4), and the weight function $w(x) = \phi(x)$ is chosen to be the mother basis function.

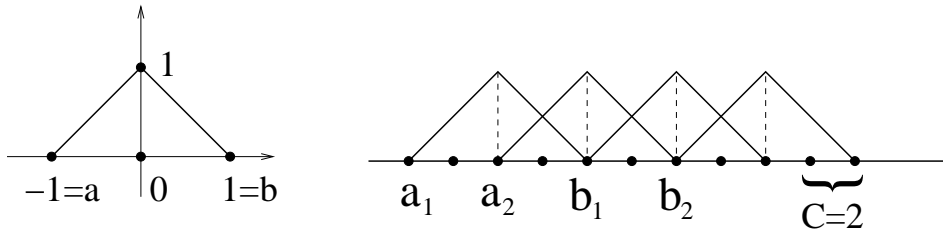


Figure 1: The mother hat function (left) with $b - a = 2$ and the location of the quadrature points (right) with $C = 2$. There are 5 quadrature points in the support of each hat function: $r + 1 = C(b - a) + 1 = 5$. Each additional basis function added on the right requires only $C = 2$ new quadrature points – the other 3 points are shared with its neighbours on the left.

3.2 The gain in computational cost

Assume that one requires the evaluation of integrals of the form (3.1) for a range of values n , for which the function f , defined by (3.2), is a smooth function (i.e., there are no corners on the corresponding part of Γ and the integrals I_n are not singular). Expressions (3.4) and (3.6) show that the scheme requires the evaluation of f at the points

$$x_{n,j} = \frac{a + j \frac{b-a}{r} + n}{N}. \quad (3.7)$$

If r is chosen such that the number of quadrature points per unit interval

$$C := \frac{r}{b-a} \quad (3.8)$$

is an integer, then one sees from (3.7) that many of the points $x_{n,j}$ coincide, and the corresponding function evaluations can be shared. This is illustrated in Figure 1 for hat functions. In particular, assume one wants to compute I_1, \dots, I_P . The evaluation of the quadrature rule for each integral individually requires

$$E_{ind} := P(r + 1) = P(C(b - a) + 1)$$

evaluations of f , i.e., $r + 1$ per integral. Reusing function evaluations, one requires only

$$E_{shared} := C(b - a) + 1 + (P - 1)C$$

evaluations of f . The first integral requires $C(b - a) + 1$ evaluations as before, but each additional integral only requires C additional function evaluations. One can choose $r = b - a$, leading to $C = 1$. With this choice, each additional evaluation of an integral only requires one additional evaluation of f .

In those parts of the discretization matrix where the smoothness assumptions about f are valid, the elements of the collocation matrix can be computed with a total number of evaluations of f that is close to the number of elements in the matrix. Note however that one still has to perform the summation in (3.6) for each integral. Assuming that the evaluation of the Green's function is costly, this summation is a cheap operation.

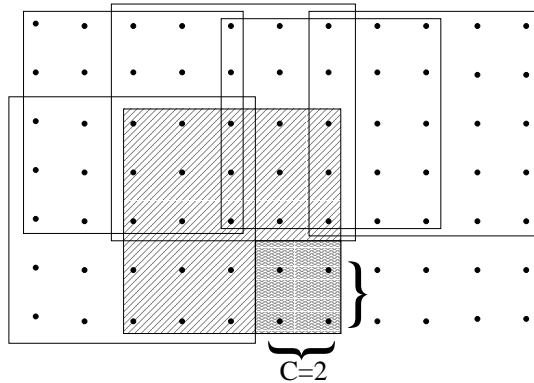


Figure 2: The location of the quadrature points in two dimensions with $b - a = 2$ and $C = 2$. Each rectangle corresponds to one double integral and contains 25 points. Once the Green's function is evaluated in all points in the rectangles on the top row and the left row, each additional rectangle requires only $C^2 = 4$ new function evaluations.

3.3 The construction of Newton-Cotes quadrature rules

The quadrature points x_j and weights w_j of the Newton-Cotes quadrature rule (3.4) need to be computed only once for each basis function $\phi(x)$. The equispaced quadrature points x_j are already known. The weights w_j are found by requiring that the integration is exact for all polynomials up to degree r . This corresponds to the following conditions

$$\sum_{j=0}^r w_j x_j^p = \int_a^b \phi(x) x^p dx, \quad p = 0, \dots, r. \quad (3.9)$$

This leads to a small system of $r + 1$ equations and $r + 1$ unknowns w_j . The construction only requires the knowledge of the moments of $\phi(x)$ in the right hand side of (3.9).

If the basis functions ϕ_n are not shifted versions of the same mother function $\phi(x)$, then the scheme can still be applied, but the weights w_j of the Newton-Cotes quadrature rule have to be computed once for each basis function ϕ_n with a different shape.

The number of quadrature points $r + 1$ determines the order of the quadrature rule [8]. Naturally, the more quadrature points, the more accurate the approximation. Higher accuracy can be achieved here by choosing a large C . In that case $r = C(b - a)$ is a larger integer multiple of $b - a$. We remark that, in general, Newton-Cotes rules of high order can be numerically unstable and the system of equations (3.9) becomes ill-conditioned [16, 10]. This turns out not to be an issue for our purposes.

3.4 Tensor-product generalization

The approach for one-dimensional integrals can easily be extended to multivariate integrals. Consider double integrals of the form

$$I_{m,n} = \int_{a_m}^{b_m} \left(\int_{a_n}^{b_n} f(t, \tau) \phi_n(\tau) d\tau \right) \phi_m(t) dt, \quad (3.10)$$

which correspond to the integrals of the Galerkin scheme in (2.3) with

$$f(t, \tau) = G(\kappa(t), \kappa(\tau))|\kappa'(\tau)||\kappa'(t)|. \quad (3.11)$$

Using the same Newton-Cotes quadrature rule as in §3.1, both for the integration in t as the integration in τ , leads to the approximation

$$I_{m,n} \approx \frac{1}{N^2} \sum_{j=0}^r \sum_{l=0}^r w_j w_l f\left(\frac{x_j + m}{N}, \frac{x_l + n}{N}\right).$$

The cost for each additional integral is now C^2 function evaluations when evaluations for t and τ are shared, compared to $(r+1)^2$ when they are not. This is illustrated in Figure 2 for the case $C = 2$ and $b - a = 2$. It remains possible to choose $r = b - a$, and hence $C = C^2 = 1$. Again, the cost of evaluating an additional double integral is only one additional evaluation of the Green's function.

4 The efficient evaluation of diagonal entries

Using the techniques of the previous section, a large part of the discretisation matrices can already be computed efficiently. There are only cN elements on or near the diagonal that correspond to singular integrals, where c is a small constant that depends on the size of the support $[a, b]$ of the mother basis function ϕ . It may be tolerable to compute these remaining elements one by one. Still, they can also be computed efficiently with a technique related to the one discussed above, but slightly more complicated.

4.1 One-dimensional singular integrals

Singular functions are not well approximated by polynomials, and hence Newton-Cotes quadrature rules are not very accurate for such functions. One solution is to include the singularity into the weight function. Assume that a singular function $u(x)$ is known in the form

$$u(x) = p(x)s(x - x_0) + q(x), \quad (4.1)$$

where $s(x - x_0)$ is singular at the point x_0 . The functions $p(x)$ and $q(x)$ are non-singular and smooth on the intervals $[a, x_0]$ and $[x_0, b]$. For example, we could have $q(x) = |x - x_0|$. The Green's function (2.2) for Helmholtz equations can be written as

$$\frac{i}{4} H_0^{(1)}(k|\kappa(t) - \kappa(\tau)|) = -\frac{2\pi}{4} J_0(k|\kappa(t) - \kappa(\tau)|) \log(|t - \tau|) + P(t, \tau), \quad (4.2)$$

where $J_0(z)$ is the Bessel function of the first kind and $P(t, \tau)$ is a non-singular function that behaves as $|t - \tau|$ when $t \approx \tau$. Thus, expression (4.2) satisfies our assumptions on the singular behaviour of the Green's function.

With $x_0 \in [a, b]$, we can write a one-dimensional singular integral on $[a, b]$ as

$$\begin{aligned} \int_a^b u(x)\phi(x) dx &= \int_a^{x_0} p(x)s(x - x_0)\phi(x) dx + \int_{x_0}^b p(x)s(x - x_0)\phi(x) dx \\ &\quad + \int_a^{x_0} q(x)\phi(x) dx + \int_{x_0}^b q(x)\phi(x) dx. \end{aligned}$$

Our approach is to construct quadrature rules for each of these four integrals. These rules necessarily depend on the value of x_0 . In a collocation method, x_0 corresponds to the singularity at the collocation point. A natural assumption in this setting is that $x_0 \in [a, b]$ is an integer. It can be seen in Figure 1 that, for the hat functions, this corresponds precisely to choosing collocation points at the peaks of the hat functions. For more general basis functions such as B-splines, these collocation points correspond to the knots of the spline.

We are led to the following set of quadrature rules:

$$\begin{aligned} \int_a^{a+j} p(x)s(x-x_0)\phi(x) dx &\approx Q_{1j}[p] := \sum_{l=0}^{r_{1jl}} w_{1jl}p(x_{1jl}), & j = 1, \dots, b-a, \\ \int_{a+j}^b p(x)s(x-x_0)\phi(x) dx &\approx Q_{2j}[p] := \sum_{l=0}^{r_{2jl}} w_{2jl}p(x_{2jl}), & j = 0, \dots, b-a-1, \\ \int_a^{a+j} q(x)\phi(x) dx &\approx Q_{3j}[p] := \sum_{l=0}^{r_{3jl}} w_{3jl}p(x_{3jl}), & j = 1, \dots, b-a, \\ \int_{a+j}^b q(x)\phi(x) dx &\approx Q_{4j}[p] := \sum_{l=0}^{r_{4jl}} w_{4jl}p(x_{4jl}), & j = 0, \dots, b-a-1. \end{aligned}$$

A detailed account of the construction of such rules is given in [10]. We choose the same grid of $r+1$ equidistant points on $[a, b]$ as before. For each of the four families of quadrature rules above, only the grid points that lie in $[a, a+j]$ or $[a+j, b]$ are used. Thus, function evaluations of the functions p and q can again be shared.

A remark concerning the accuracy of these rules should be made here. Since the intervals $[a, a+j]$ and $[a+j, b]$ are smaller than $[a, b]$, they contain less quadrature points. As a consequence, the order of the quadrature rule is lower. For example, the integral on the interval $[a, a+1]$ will be evaluated using just $C+1$ quadrature points. It may be beneficial to choose $C > 1$ in this case.

4.2 Two-dimensional singular integrals

First, we assume a singular function $u(x, y)$ with a known singular behaviour,

$$u(x, y) = p(x, y)s(x-y) + q(x, y).$$

The function $s(x-y)$ is singular when $x = y$. The functions $p(x, y)$ and $q(x, y)$ are non-singular everywhere and smooth everywhere except possibly at $x = y$. The singular behaviour of the Green's function for the Helmholtz equation, given in (4.2), satisfies these assumptions. Our goal is to use only evaluations of $p(x, y)$ and $q(x, y)$ at precisely the same grid points as shown in Figure 2, so that the function values can be shared among neighbouring elements of the discretization matrix.

We can write the double integral (3.10) as an integration on $[a, b] \times [a, b]$,

$$I_{m,n} = \frac{1}{N^2} \int_a^b \int_a^b f\left(\frac{x+m}{N}, \frac{y+n}{N}\right) \phi(x)\phi(y) dy dx.$$

The integration domain is shown in Figure 3. The integrand is singular when $x+m = y+n$, or $x = y - \delta$ with $\delta = m - n$.

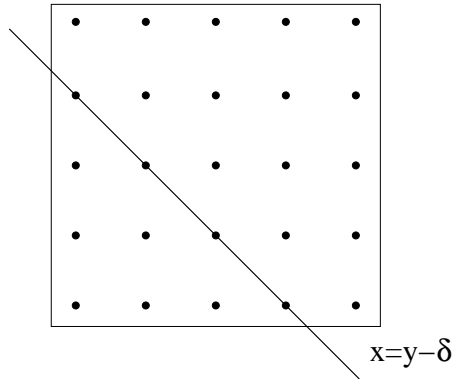


Figure 3: The integration domain for one singular double integral. The domain is divided into two parts by the singularity along the line $x = y - \delta$. The constant $\delta = m - n$ is the shift between the basis functions $\phi_n(x)$ and $\phi_m(y)$.

For convenience of notation, we write the double integral in the following model form

$$I_\delta := \int_a^b \int_a^b (p(x, y)s(x - y + \delta) + q(x, y))\phi(x)\phi(y) \, dy \, dx,$$

where δ represents a shift of the singularity line that depends on the distance between the two basis functions. Here, the functions p and q are smooth on the two parts on either side of the line of singularities in Fig. 3, but not across that line.

Unlike in the non-singular case, a tensor-product generalization of the one-dimensional approach is not straightforward. In order to illustrate the issue, consider the following one-dimensional function that corresponds to the inner integral of I_δ ,

$$v(x) := \int_a^b (p(x, y)s(x - y + \delta) + q(x, y))\phi(y) \, dy.$$

One can use the technique of the one-dimensional case to approximate this integral. However, the result is again a singular function. In general it is very difficult, or even impossible, to explicitly separate the singular and non-singular part of $v(x)$ analytically. It is therefore not possible to apply the one-dimensional approach a second time. For this reason, we proceed by constructing a two-dimensional cubature rule for I_δ .

Divide the integration domain into two parts, Δ_1 and Δ_2 , corresponding to the upper and lower region in Fig. 3. For each value of δ , we will construct four cubature rules that are exact for the case where p or q are bivariate polynomials. There are $2C(b - a) + 1$ possible values of δ . (Note that in Fig. 3, there are $9 = 2 \cdot 2 \cdot 2 + 1$ possible lines parallel to the line

shown that cross at least one quadrature point.) The cubature rules are

$$\begin{aligned} \int_{\Delta_1} p(x, y) s(x - y + \delta) \phi(x) \phi(y) dx dy &\approx Q_{\delta_1}^c[p] := \sum_j w_{\delta_1 j}^c p(\mathbf{x}_{\delta_1 j}), \\ \int_{\Delta_2} p(x, y) s(x - y + \delta) \phi(x) \phi(y) dx dy &\approx Q_{\delta_2}^c[p] := \sum_j w_{\delta_2 j}^c p(\mathbf{x}_{\delta_2 j}), \\ \int_{\Delta_1} q(x, y) \phi(x) \phi(y) dx dy &\approx Q_{\delta_3}^c[p] := \sum_j w_{\delta_3 j}^c p(\mathbf{x}_{\delta_3 j}), \\ \int_{\Delta_2} q(x, y) \phi(x) \phi(y) dx dy &\approx Q_{\delta_4}^c[p] := \sum_j w_{\delta_4 j}^c p(\mathbf{x}_{\delta_4 j}). \end{aligned}$$

We obtain I_δ as the sum of these four approximations.

The set of cubature points are the points of the regular grid, shown in Fig. 3, that lie in the domain Δ_1 or Δ_2 respectively. For each rule, we will require exactness for polynomials up to a certain degree in x and y . That is, for certain combinations of integers k and l , we require

$$Q_{\delta_1}^c[x^k y^l] = \int_{\Delta_1} x^k y^l s(x - y + \delta) \phi(x) \phi(y) dy dx. \quad (4.3)$$

Similar relations hold for the other rules. We choose the polynomials from the sequence

$$1, x, y, x^2, xy, y^2, x^3, x^2y, xy^2, y^3, \dots$$

For a rule with q points, we truncate this sequence after q terms. This choice has the beneficial property of maximizing the order of the resulting cubature rule [6]. Conditions (4.3) lead to a linear system of equations that can be used to solve for the weights $w_{\delta_1 j}^c$.

We remark that, as in the one-dimensional case, some cubature rules may have very few cubature points. At the same time, these rules correspond to small integration domains. In our numerical experiments this has not led to any significant loss of accuracy compared to the rules with more points on larger domains.

Finally, we note that in our implementation we have computed the required moments, given by singular double integrals themselves in the right hand side of (4.3), using the general purpose integration package Cubpack [7]. The cubature rules depend on the basis functions and on the type of singularity of the Green's function (for example a logarithmic singularity). They do not depend on the shape of the domain Γ , on $G(\mathbf{x}, \mathbf{y})$ itself or on the number of basis functions N . Hence, they need be computed only once.

4.3 Domains with corners

Ideally, every integrand that was encountered in this paper is smooth everywhere on the boundary Γ except possibly at points of singularity when $x = y$. For domains Γ with corners, this is not necessarily the case. The integrand is typically continuous but not differentiable at the corner points. Therefore, the accuracy of the Newton-Cotes quadrature will degrade, though not all accuracy is lost.

The problem could be addressed in exactly the same way as for the singularity. A corner divides the integration domain into two parts. Compared to Fig. 3, the line of separation is

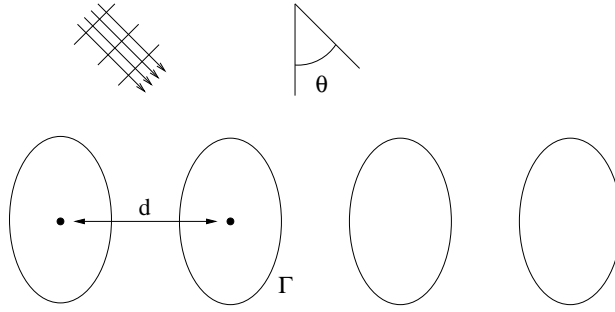


Figure 4: A periodic grid of scattering obstacles with period d . The incoming plane wave makes an angle θ with the normal direction.

either horizontal or vertical in this case. Quadrature or cubature rules can be constructed for both domains separately. For a very small number of entries in the discretization matrix, there can be a horizontal, a vertical and a diagonal line in one rectangle. These entries correspond to singular integrals where both basis functions contain a corner in their support. There is only a limited number of such entries per corner of the domain Γ .

Though nothing prevents us from constructing cubature rules tailored for such configurations, the number of required rules multiply and the result may be rather cumbersome. We will not pursue that approach in this paper. Like the number of singular integrals, the total number of entries in the discretization matrix that is affected by a corner point is cN , where c is again a constant that depends on the size of the support of the basis functions. In our implementation we have currently chosen to compute these elements using other means. There is a trade-off between additional preprocessing computational time, required for the construction of suitable quadrature and cubature rules, and additional running time for simulations.

5 Scattering by diffraction gratings

In this section we will apply the method discussed above to the problem of scattering by diffraction gratings. In this application, the Green's function is given by a slowly convergent series. First, we accelerate the convergence of the series, thereby reducing the time required to evaluate the Green's function. Next, we show that even with this acceleration procedure, the possibility of sharing function evaluation leads to large savings in computational times.

5.1 A quasi-periodic Green's function

The propagation and scattering of time-harmonic TM-polarized electromagnetic waves is described by the Helmholtz equation. We consider the scattering of such waves in two dimensions by a periodic grid of obstacles, as shown in Figure 4. An incident plane wave makes an angle θ with respect to the normal direction. It is shown in [17] that this leads to a quasi-periodic Green's function given by a series of images,

$$G_d(\mathbf{x}, \mathbf{y}) = \sum_{m=-\infty}^{\infty} \frac{i}{4} H_0^{(1)}(k|\mathbf{x} - \mathbf{y} + m\mathbf{d}|) e^{im\beta d}. \quad (5.1)$$

The vectors $\mathbf{x}, \mathbf{y} \in \mathbb{R}^2$ are the field point and source point respectively. The vector $\mathbf{d} = [d \ 0]^T$ represents the displacement of each consecutive obstacle. The factor $e^{im\beta d}$, with $\beta = k \sin \theta$, accounts for a phase difference on each shifted obstacle. The integral equation to solve is an integral equation of the first kind,

$$\int_{\Gamma} G_d(\mathbf{x}, y) u(y) ds_y = -e^{ik\alpha \mathbf{x}}, \quad x \in \Gamma, \quad (5.2)$$

with $\alpha = [\cos(3\frac{\pi}{2} + \theta) \ \sin(3\frac{\pi}{2} + \theta)]^T$. For an in-depth description of diffraction gratings, the reader is referred to [17]. Integral equation methods for these problems have previously been described in, e.g., [3, 15].

5.2 A new integral representation

The series (5.1) converges very slowly – its terms decay as $O(m^{-\frac{1}{2}})$. A review of efficient evaluation techniques for quasi-periodic Green’s functions is given in [14], including lattice sums, Ewald’s method and integral representations. A novel method, that remains highly accurate even for very large wavenumbers, was recently proposed in [13]. Here, we propose a different approach from those mentioned in [13, 14]. The advantage of our approach is that it leads to a straightforward and efficient implementation, subject only to a certain nonresonance condition that will be clearly indicated.

First, the infinite sum is rewritten as a contour integral in the complex plane (the integral representation differs from those in [14]). The contour integral is constructed such that the sum of the residues of all poles in the interior of the contour, multiplied by the factor $2\pi i$, evaluates exactly to the infinite sum. Thus, by the residue theorem, the limit of the infinite sum and the value of the integral are identical [1]. The problem is now reduced to the evaluation of a complex line integral. We choose a particularly simple contour, a straight line parallel to the imaginary axis, and we show that the trapezoidal rule converges exponentially quickly to the desired value. The simplicity of the trapezoidal rule means that the final result is obtained by summing a number of evaluations of the integrand, leading to simple and explicit formulas.

We define the functions

$$\begin{aligned} C^M(\mathbf{x}, \mathbf{y}) &= \sum_{m=-M}^M \frac{i}{4} H_0^{(1)}(k|\mathbf{x} - \mathbf{y} + m\mathbf{d}|) e^{im\beta d}, \\ L^M(\mathbf{x}, \mathbf{y}) &= \sum_{m=-\infty}^{-M-1} \frac{i}{4} H_0^{(1)}(k|\mathbf{x} - \mathbf{y} + m\mathbf{d}|) e^{im\beta d}, \\ R^M(\mathbf{x}, \mathbf{y}) &= \sum_{m=M+1}^{\infty} \frac{i}{4} H_0^{(1)}(k|\mathbf{x} - \mathbf{y} + m\mathbf{d}|) e^{im\beta d}, \end{aligned}$$

such that $G_d = C^M + L^M + R^M$ for any $M \in \mathbb{N}$. The function C^M requires $2M + 1$ evaluations of the Hankel function. We will implement this function by explicitly summing these terms (using $M = 1$ in all subsequent computations, unless noted otherwise). The infinite sums L^M and R^M will be evaluated based on the following theorem.

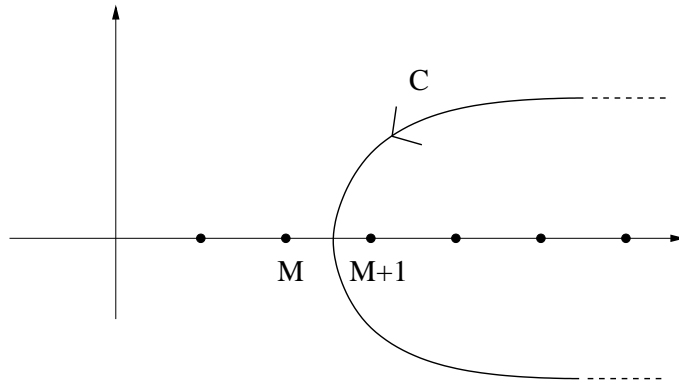


Figure 5: The integral along the contour C encircles poles at all integers larger than M .

Theorem 5.1. *Let C be a contour as shown in Figure 5 that crosses the real line at a point $t \in (M, M + 1)$ and let s be any odd integer. Then the following identity holds*

$$R^M(\mathbf{x}, \mathbf{y}) = \frac{1}{2\pi i} \int_C \frac{i}{4} H_0^{(1)}(k|\mathbf{x} - \mathbf{y} + m\mathbf{d}|) e^{im\beta d} \frac{\pi}{\sin(\pi m)} e^{i\pi m s} dm, \quad (5.3)$$

for any $\mathbf{x}, \mathbf{y} \in \mathbb{R}^2$ with $|\mathbf{x} - \mathbf{y}| < Md$.

Proof. Since $|\mathbf{x} - \mathbf{y}| < Md$ and $|m\mathbf{d}| > Md$, for all m in C and its interior, we have $|\mathbf{x} - \mathbf{y} + m\mathbf{d}| > 0$. Thus, the contour integral does not contain the singularity of the Hankel function. The integrand is therefore analytic in the interior of C , except at poles of the integrand. Hence, by the residue theorem, the value of the contour integral is given by the sum of the residues of the integrand at these poles, multiplied by $2\pi i$ [1].

The function $\frac{\pi}{\sin(\pi m)}$ has poles at the points $m \in \mathbb{Z}$ with residue $(-1)^m$. For any odd integer s we have $e^{i\pi m s} = (-1)^m$. It follows that, at a pole $m \in \mathbb{Z}$, the residue of the integrand in (5.3) is given by

$$\text{Res} \left\{ \frac{i}{4} H_0^{(1)}(k|\mathbf{x} - \mathbf{y} + m\mathbf{d}|) e^{im\beta d} \frac{\pi}{\sin(\pi m)} e^{i\pi m s} \right\} = \frac{i}{4} H_0^{(1)}(k|\mathbf{x} - \mathbf{y} + m\mathbf{d}|) e^{im\beta d}.$$

Summing up all the residues at the poles $m = M + 1, M + 2, \dots$ now proves the result. \square

We are still free to choose the contour C and the precise value of the odd integer s . For simplicity, we consider a line parallel to the imaginary axis. This line is parameterized by

$$m(p) = M + \frac{1}{2} + ip, \quad p \in (-\infty, \infty),$$

such that we can formally write, after substituting $m'(p) = i$ and simplifying,

$$R^M(\mathbf{x}, \mathbf{y}) = -\frac{i}{8\pi} \int_{-\infty}^{\infty} H_0^{(1)}(k|\mathbf{x} - \mathbf{y} + m(p)\mathbf{d}|) e^{im(p)\beta d} \frac{\pi}{\sin(\pi m(p))} e^{i\pi m(p)s} dp.$$

The integer s will be chosen such that the integrand decays rapidly away from the real line at $p = 0$. We note that, like the exponential function e^{iz} , the Hankel function $H_0^{(1)}(z)$ becomes

exponentially small for complex z with increasingly positive imaginary part and exponentially large for complex z with increasingly negative imaginary part. The function $\frac{\pi}{\sin(\pi m)}$ decays exponentially in both directions away from the real axis (which, in fact, is precisely the reason it was introduced here). From the asymptotic behaviour of the Hankel function for large arguments [2], one can verify that the integrand $I(p)$ behaves like

$$I(p) \sim e^{-kdp} e^{-\beta dp} e^{-\pi|p|} e^{-\pi sp}, \quad p \rightarrow \infty. \quad (5.4)$$

Exponential decay is guaranteed for positive and negative p only for the contribution $e^{-\pi|p|}$ of the $\frac{\pi}{\sin(\pi m)}$ function. The other factors either decay or grow exponentially quickly, depending on the sign of p . We can choose s to neutralize the term $e^{-kdp} e^{-\beta dp}$ as much as possible. An optimal choice is

$$s := \begin{cases} \left\lfloor -\frac{kd+\beta d}{\pi} \right\rfloor, & \text{if } \left\lfloor -\frac{kd+\beta d}{\pi} \right\rfloor \text{ is odd,} \\ \left\lfloor -\frac{kd+\beta d}{\pi} \right\rfloor + 1, & \text{otherwise.} \end{cases} \quad (5.5)$$

Here, $\lfloor a \rfloor$ denotes the largest integer smaller than a . Define the difference

$$D := -kd - \beta d - \pi s. \quad (5.6)$$

The integrand behaves as $I(p) \sim e^{-\pi|p|} e^{Dp}$. There is an exponential decay for increasing $|p|$ if $|D| < \pi$. With the above choice of s , we have

$$-\pi \leq D < \pi.$$

The leftmost inequality becomes an equality when

$$\exists n \in \mathbb{Z} : \quad -\frac{kd + \beta d}{\pi} = 2n. \quad (5.7)$$

To summarize, the integral representation (5.3), with C taken parallel to the imaginary axis and with s chosen as in (5.5), has an integrand that decays exponentially quickly in both directions away from the real line. There is no such decay for some exceptional values of k , namely when (5.7) is satisfied. Taking into account that $\beta = k \sin(\theta)$, we exclude this case by imposing the *nonresonance* condition,

$$\forall n \in \mathbb{Z} : \quad kd \frac{1 + \sin \theta}{\pi} \neq 2n. \quad (5.8)$$

One can verify that for combinations of k , d and θ that do not satisfy the nonresonance condition, the terms in the infinite series are in fact not oscillatory. This motivates the name of the condition. For the sake of brevity, we do not explore further the case of resonant values of k . In the remainder of this paper, we assume that the nonresonance condition is satisfied. Finally, we note that the integral representation of the function L^M is entirely analogous.

5.3 Efficient evaluation using the trapezoidal rule

With the optimal choice of the odd integer s , the integral on a line parallel to the imaginary axis is well defined and suitable for numerical integration. It is well known that the trapezoidal rule converges exponentially for smooth and rapidly decaying integrands on $(-\infty, \infty)$. We approximate R^M by

$$R^M(\mathbf{x}, \mathbf{y}) \approx -\frac{ih}{8\pi} \sum_{l=1}^Q H_0^{(1)}(k|\mathbf{x} - \mathbf{y} + m_l \mathbf{d}|) e^{im_l \beta d} \frac{\pi}{\sin(\pi m_l)} e^{i\pi m_l s}. \quad (5.9)$$

Here, the Q quadrature points m_l form an equidistant grid on the line in the complex plane with real part $M + \frac{1}{2}$. We restrict the imaginary part to the interval $[T_L, T_R]$. The grid length is then $h = \frac{T_R - T_L}{Q-1}$ and we have

$$m_l := M + \frac{1}{2} + i \left(T_L + \frac{l-1}{Q-1} (T_R - T_L) \right), \quad l = 1, \dots, Q. \quad (5.10)$$

We can use the knowledge about the behaviour of the integrand to find a suitable truncation from the infinite interval $(-\infty, \infty)$ to the finite interval $[T_L, T_R]$. Since the integrand behaves as $I(p) \sim e^{-\pi|p|} e^{Dp}$, we choose

$$T_L := \frac{\log(\epsilon)}{D + \pi}, \quad \text{and} \quad T_R := \frac{\log(\epsilon)}{D - \pi}, \quad (5.11)$$

where ϵ is the desired accuracy. These values are such that the integrand has roughly reached the small value ϵ where the integration domain is truncated.

The explicit procedure to evaluate $R^M(\mathbf{x}, \mathbf{y})$ is as follows. Given k , d and θ :

1. Determine the optimal value of s from expression (5.5).
2. Compute the constant D , that characterises the exponential decay of the integrand, from the expression (5.6).
3. Compute the boundaries of the interval $[T_L, T_R]$ from (5.11).
4. Evaluate the sum (5.9) using the Q quadrature points (5.10).

The procedure for computing $L^M(\mathbf{x}, \mathbf{y})$ is entirely analogous. The function $C^M(\mathbf{x}, \mathbf{y})$ is computed by explicit summation.

6 Numerical results

We will first illustrate the performance of our approach to evaluate the quasi-periodic Green's function itself in Section 6.1. Next, we illustrate the total number of function evaluations that are required for the construction of a discretization matrix in Section 6.2. We focus our attention on the Galerkin discretization, as that is the most challenging case.

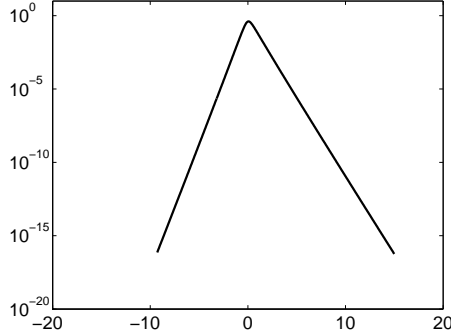


Figure 6: The size of the integrand for evaluating the Green's function, along the contour in the complex plane as a function of the imaginary part p . The integration domain $(-\infty, \infty)$ is truncated to $[T_L, T_R]$ where the integrand becomes smaller than machine precision.

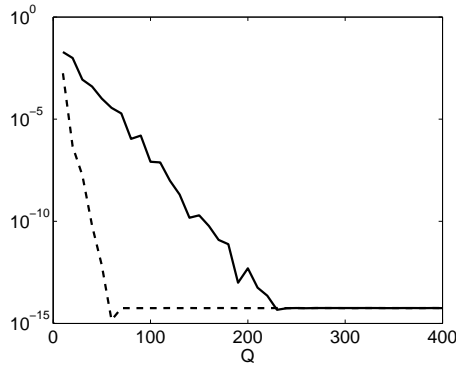


Figure 7: Convergence of the trapezoidal rule as a function of Q ($x = [0 \ 0]^T$, $y = [0 \ 0.01]^T$, $k = 3$, $d = 2$, $\theta = \pi/6$, $M = 1$). The dashed line shows the result after the sinh-transformation.

6.1 Evaluation of the Green's function

We evaluate the quasi-periodic Green's function (5.1) using the trapezoidal rule (5.9). A typical plot of the integrand is shown in Figure 6. The integrand decays exponentially away from the point $p = 0$ that correspond to the point on the real axis. The slope of the decay is different in the two directions away from $p = 0$, into the upper and lower halves of the complex plane, as predicted by the theory.

Following [14], we choose the points $x = [0 \ 0]^T$ and $y = [0 \ 0.01]^T$ for numerical tests. Figure 7 shows the convergence of the trapezoidal rule for evaluating $G_d(\mathbf{x}, \mathbf{y})$ for $k = 2$, $d = 1$ and $\theta = \pi/6$. The computation of C^M requires 3 evaluations for the choice $M = 1$. We use Q quadrature points for both L^M and R^M . It is clear that the approximation converges at an exponential rate as a function of Q . The smallest absolute error is $4.6e - 15$ at $Q = 230$. The relative error at that point is $8.8e - 15$. All computations were performed in Matlab using double precision.

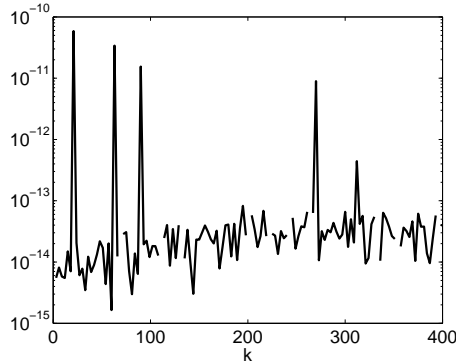


Figure 8: Convergence of the trapezoidal rule as a function of k for fixed $Q = 80$ after a sinh transformation. The spikes are values of k that are close to resonance points.

A well-known technique for accelerating the convergence of the trapezoidal rule for rapidly decaying function is the so-called sinh-transformation [8]. The results of applying the trapezoidal rule after the sinh-transformation is shown with the dashed line in the same Figure. In this case, the minimal error is obtained using just 60 quadrature points.

Figure 8 shows the absolute error as a function of increasing wavenumber k , while keeping Q fixed. The spikes that are visible in the figure correspond to values of k that are close to resonance values. The approximation appears to degrade with increasing the values of k , but only very slightly. In that sense, this method for oscillatory sequences is quite different from methods for oscillatory integrals for evaluating an integral of an oscillatory Hankel function or exponential, rather than an infinite sum. For such integrals, one can construct methods that improve rapidly with increasing k [11, 12].

We note that for very large values of the wavenumber k , the method should be implemented with care. In particular, the summation in (5.9) may become numerically unstable. The integrand in the integral representation (5.3) still exhibits exponential decay along the suggested integration contour. However, this decay is an asymptotic result and the integrand can become very large before the asymptotic behaviour sets in. As a result, some of the terms in the summation (5.9) are large in absolute value and loss of accuracy can be expected due to cancellation errors. This issue is entirely avoided by choosing a larger M (as shown in Fig. 5). This means that for large values of k one has to explicitly sum up more terms of the oscillatory series. The integral representation can then be used for the remainder of the series. This leads to numerically stable computations when M is sufficiently large.

6.2 Scattering by a diffraction grating

We chose a periodic grid of ellipse-shaped obstacles, as shown in Figure 4, with radii 0.3 and 0.5 respectively. With a periodicity constant $d = 1$, the gap between two consecutive ellipses in the horizontal direction is 0.4. The wavenumber $k = 15$ was chosen such that this gap is approximately one half wavelength. The incoming wave is incident at $\theta = \pi/6$. Fig. 9 shows the solution of the integral equation (5.2) in this configuration.

The computing times in our experiments are completely dominated by the time required to

N	$C = 1$			$C = 2$		
	E	E/N^2	RelErr	E	E/N^2	RelErr
32	1,386	1.35	$2.1E - 2$	5,208	5.09	$4.0E - 4$
64	4,810	1.17	$1.3E - 3$	18,584	4.54	$7.0E - 6$
128	17,802	1.09	$8.6E - 5$	69,912	4.27	$3.3E - 7$
256	68,362	1.04	$2.9E - 5$	270,872	4.13	$1.6E - 7$
512	267,786	1.02	$1.6E - 5$	1,066,008	4.07	$8.2E - 8$
1024	1,059,850	1.01	$9.0E - 6$	4,229,144	4.03	$4.3E - 8$

Table 1: The total number of evaluations E of the Green’s function in a Galerkin discretization for different values of C . The ratio E/N^2 should approach C^2 . RelErr is the maximal relative error in the matrix entries due to the quadrature approximation.

evaluate the Green’s function. Even with the efficient representation described above, evaluating the Green’s function remains the bottleneck in this application. For that reason, the most informative result is the total number of function evaluations required for the construction of a discretization matrix.

These results are shown in Table 1. The table shows the total number of evaluations E of the Green’s function required for constructing a Galerkin discretization matrix. This number corresponds exactly to the number of infinite sums that were computed in the implementation. The second column shows the ratio E/N^2 , where N^2 is the number of matrix entries. According to the theory, this ratio should approach C^2 . The accuracy of the quadrature approximation is measured by computing the following relative error,

$$RelErr := \frac{\|A_g - \tilde{A}_g\|}{\|A_g\|},$$

where A_g is the exact Galerkin matrix and \tilde{A}_g is the approximation by quadrature. The accuracy improves for increasing values of N because the support of the basis functions becomes smaller. As expected, the results for $C = 2$ are more accurate because more quadrature points are used per matrix entry. With this choice a total number of approximately $4N^2$ function evaluations are required.

Finally we note that, for $C = 1$, we indeed have approximately $E \approx N^2$ function evaluations. For the case $N = 1024$, computing one million regular and singular double integrals requires approximately one million costly function evaluations.

7 Conclusions

The implementation of boundary element methods typically requires the evaluation of a large number of integrals, at least one for each element in the discretization matrix. We described an efficient quadrature scheme in which evaluations of the Green’s function are maximally reused, by sharing them among the computations of neighbouring matrix entries. With an optimal choice of parameters, we showed that the computation of one matrix entry requires only one additional evaluation of the Green’s function. This remains true even when matrix entries are given by singular two-dimensional integrals. As a result, the computation

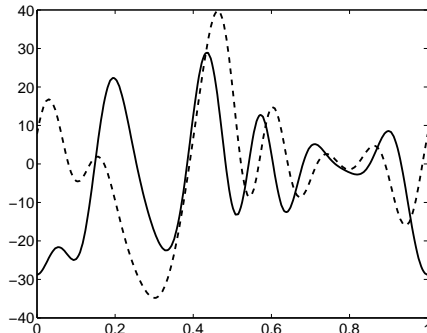


Figure 9: Real part (solid line) and imaginary part (dashed line) of the solution for a periodic grid of ellipse-shaped obstacles at distances $d = 1$ (with $k = 15$). The parameterization maps $[0, 1]$ to the ellipse in anti-clockwise direction, starting at the rightmost point on the ellipse.

time required for constructing the discretization matrix becomes almost independent of the chosen discretization scheme: a Galerkin method, which requires evaluating many double integrals, can be implemented as efficiently as a Nyström method, which requires no numerical integration at all.

The increased efficiency comes at a cost of having to compute a small set of quadrature rules a priori. These rules depend on the chosen basis functions. They do not depend on the geometry of the problem however, so they have to be computed only once. A second disadvantage of the approach is that the sharing of function evaluations is most effective only when the integral equation is discretized on a regular grid. We note that this restriction too is not as severe as it may appear. The technique can still be applied if, for example, only part of the grid is regular. Moreover, it appears that many kinds of deviations from a regular grid can be compensated for, at least in principle, by computing a larger set of quadrature rules a priori. Such generalizations are particularly challenging in three-dimensional problems and are a topic of further research.

References

- [1] M. J. Ablowitz and A. S. Fokas. *Complex variables: introduction and applications*. Cambridge University Press, Cambridge, 1997.
- [2] M. Abramowitz and I. A. Stegun. *Handbook of mathematical functions with formulas, graphs, and mathematical tables*. Dover Publications, New York, 1965.
- [3] T. Arens, S. N. Chandler-Wilde, and J. A. DeSanto. On integral equation and least square methods for scattering by diffraction gratings. *Communications in Computational Physics*, 1(6):1010–1042, 2006.
- [4] K. E. Atkinson. *The numerical solution of integral equations of the second kind*. Cambridge University Press, Cambridge, 1997.

- [5] D. Colton and R. Kress. *Integral equation methods in scattering theory*. Wiley, New York, 1983.
- [6] R. Cools. Constructing cubature formulae: The science behind the art. *Acta Numerica*, 6:1–54, 1997.
- [7] R. Cools and A. Haegemans. Algorithm 824: CUBPACK: A package for automatic cubature; framework description. *ACM Trans. Math. Softw.*, 29(3):287–296, 2003.
- [8] P. J. Davis and P. Rabinowitz. *Methods of numerical integration*. Computer Science and Applied Mathematics. Academic Press, New York, 1984.
- [9] R. F. Harrington. *Field computation by moment methods*. Macmillan, New York, 1968.
- [10] D. Huybrechs and S. Vandewalle. Composite quadrature formulae for the approximation of wavelet coefficients of piecewise smooth and singular functions. *J. Comput. Appl. Math.*, 180(1):119–135, 2005.
- [11] D. Huybrechs and S. Vandewalle. On the evaluation of highly oscillatory integrals by analytic continuation. *SIAM J. Numer. Anal.*, 44(3):1026–1048, 2006.
- [12] D. Huybrechs and S. Vandewalle. A sparse discretisation for integral equation formulations of high frequency scattering problems. *SIAM J. Sci. Comput.*, 2007. To appear.
- [13] H. Kurkcu and F. Reitich. Efficient calculation of Green’s functions for the two-dimensional Helmholtz equation in periodic domains. In *Proceedings of the 8th International Conference on Mathematical and Numerical Aspects of Waves*, 2007.
- [14] C. W. Linton. The Green’s function for the two-dimensional Helmholtz equation in periodic domains. *J. Engrg. Math.*, 33(4):377–401, 1998.
- [15] A. Rathsfeld, G. Schmidt, and B. H. Kleemann. On a fast integral equation method for diffraction gratings. *Commun. Comput. Phys.*, 1(6):984–1009, 2006.
- [16] W. Sweldens and R. Piessens. Quadrature formulae and asymptotic error expansions for wavelet approximations of smooth functions. *SIAM J. Numer. Anal.*, 31(4):1240–1264, 1994.
- [17] C. H. Wilcox. *Scattering theory for diffraction gratings*. Springer-Verlag, New-York, 1984.